NEW DIFFRACTION DATA

Synthesis, crystal structure, and X-ray diffraction data of lithium *m*-phenylenediamine sulfate $Li_2(C_6H_{10}N_2)(SO_4)_2$

Junyan Zhou ●,[1,2,a] Congcong Chai,[1,3] Munan Hao,[1,2] and Xin Zhong[1]

[1]*Beijing National Laboratory for Condensed Matter Physics, Institute of Physics, Chinese Academy of Sciences, Beijing 100190, China*

[2]*School of Physical Sciences, University of Chinese Academy of Sciences, Beijing 101408, China*

[3]*College of Materials Science and Opto-Electronic Technology, University of Chinese Academy of Sciences, Beijing 101408, China*

A new organic–inorganic hybrid lithium *m*-phenylenediamine sulfate (LPS), $Li_2(C_6H_{10}N_2)(SO_4)_2$, was synthesized under aqueous solution conditions. The X-ray powder diffraction study determined that the title compound crystallized in a monoclinic system at 300 K, with unit-cell parameters $a = 7.8689(6)$ Å, $b = 6.6353(5)$ Å, $c = 11.8322(10)$ Å, $\beta = 109.385(3)$ °, $V = 582.77(8)$ Å³. Indexing of the diffraction patterns collected from 100 to 600 K reveals that LPS has no structural phase transition within the measured temperature range, and the volume expansion coefficient is approximately 2.79×10^{-5} K⁻¹. The crystal structure was solved based on the single-crystal diffraction data with space group $P2_1/m$. Lithium and SO_4^{2-} are found to form quasi-two-dimensional anti-fluorite [LiSO4] layers stacking along the *c*-axis, with *m*-phenylenediamine molecules inserted in the anti-fluorite layers and forming hydrogen bonds to the SO_4^{2-}. This explains a moderate anisotropic expansion in LPS. © *The Author(s), 2021. Published by Cambridge University Press on behalf of International Centre for Diffraction Data.* [doi:10.1017/S0885715621000221]

I. INTRODUCTION

In recent years, organic–inorganic hybrids have gained worldwide research interests due to their potential applications in catalysis (Llabresixamena *et al.*, 2007), storage (Rosi *et al.*, 2003), sensing (Yanai *et al.*, 2011), ion conduction (Hurd *et al.*, 2009), nonlinear optics (Wang *et al.*, 2012), piezoelectric, and ferroelectrics (Liao *et al.*, 2019). Among organic–inorganic hybrids, the perovskite structure (Li *et al.*, 2017) composed of metal cations, protonated organic amine, and acid ions form a genre that is characterized by low cost in synthesis and great diversity in chemical composition or structure. The rich choice of cations, anions, and organic amine molecules of proper size and configuration in a specific ratio allows one to synthesize a variety of hybrid organic–inorganic perovskites (HOIPs) with different polyhedra stacking from zero to three dimensions (Saparov and Mitzi, 2016; Ju *et al.*, 2018; Chen *et al.*, 2020; Hu *et al.*, 2020). These HOIPs usually exhibit lower symmetry in structure but can be viewed as derivatives of perovskite regardless of the way cation polyhedrons are stacked. In comparison with HOIPs, organic–inorganic hybrids with other structural types are not so common and have been much less reported.

It is known that many inorganic compounds crystallize in ThCr2Si2 (Ban and Sikirica, 1965) structural type. In this structure, each chromium atom is connected to four silicon atoms to form [CrSi4] tetrahedrons, and adjacent tetrahedrons are connected in an edge sharing way to form anti-fluorite layers. The thorium atoms are intercalated in the anti-fluorite layers. In this work, we report the synthesis and structure of a new organic–inorganic hybrid lithium *m*-phenylenediamine sulfate (LPS), $Li_2(C_6H_{10}N_2)(SO_4)_2$, with a regular layered structure. LPS can be regarded as a variant of ThCr2Si2 with a lower symmetry, where thorium, chromium, and silicon atoms are replaced by protonated *m*-phenylenediamine, lithium, and sulfate ions, respectively. Our findings lead to a new structural system of organic–inorganic hybrid with anti-fluorite type layers.

II. EXPERIMENTAL

Single crystals of LPS were prepared by mixing stoichiometric ratios of lithium sulfate (60 mmol) and *m*-phenylenediamine sulfate (60 mmol) into de-ionized water (160 ml) in a 200 ml beaker to get a clear solution. After evaporation of the solvent at 80 °C, colorless crystals were obtained from the beaker.

Powder X-ray diffraction (PXRD) data were collected from 100 to 600 K on a Rigaku SmartLab diffractometer with Cu$K\alpha$ radiation (40 kV, 30 mA) and a germanium monochromator in a reflection mode ($2\theta = 5$–80°, step = 0.01° 2θ, and scan speed = 1° min⁻¹). The sample for PXRD was prepared by grinding the single crystals for 15 min to eliminate the grain-size effect. The powder was carefully scraped flat by a piece of glass to minimize the preferred orientation. To determine the crystal structure, a crystal of size $0.015 \times 0.128 \times 0.181$ mm³ was selected for the single-crystal X-ray

---

a)Author to whom correspondence should be addressed. Electronic mail: 348612272@qq.com

TABLE I. PXRD data of lithium *m*-phenylenediamine sulfate at 300 K.

$2\theta_{obs}$ (°)	d_{obs} (Å)	$(I/I_0)_{obs}$ (%)	h	k	l	$2\theta_{calc}$ (°)	d_{calc} (Å)	$\Delta 2\theta$ (°)
7.903	11.178	80	0	0	1	7.900	11.1829	0.003
15.852	5.5862	9	0	0	2	15.849	5.5872	0.003
16.351	5.4169	18	1	0	1	16.355	5.4156	−0.004
21.146	4.1980	100	1	1	1	21.148	4.1977	−0.002
22.540	3.9416	20	−2	0	1	22.549	3.9400	−0.009
23.878	3.7237	30	0	0	3	23.876	3.7239	0.001
26.274	3.3892	9	−2	1	1	26.277	3.3888	−0.003
26.537	3.3562	30	1	1	2	26.541	3.3557	−0.004
26.812	3.3224	45	0	2	0	26.813	3.3223	−0.001
27.480	3.2431	4	2	1	0	27.479	3.2433	0.002
27.680	3.2202	14	2	0	1	27.679	3.2203	0.001
27.998	3.1844	4	0	2	1	27.997	3.1844	0.000
31.572	2.83150	25	1	2	1	31.573	2.8315	0.000
32.024	2.79259	16	0	0	4	32.024	2.7925	−0.001
33.065	2.70696	16	2	0	2	33.067	2.7068	−0.002
34.343	2.60915	3	−3	0	1	34.353	2.6084	−0.010
37.967	2.36797	6	1	0	4	37.970	2.3678	−0.002
38.926	2.31184	4	2	2	1	38.923	2.3120	0.003
39.518	2.27859	5	2	0	3	39.515	2.2787	0.003
39.774	2.26448	4	3	0	1	39.772	2.2646	0.002
40.349	2.23352	9	0	0	5	40.343	2.2339	0.006
44.112	2.05134	8	−3	2	1	44.111	2.0514	0.001
45.655	1.98552	6	3	2	0	45.652	1.9857	0.003
47.048	1.92992	6	−2	3	1	47.039	1.9303	0.010
48.214	1.88596	6	1	1	5	48.218	1.8858	−0.004
52.522	1.74096	7	4	0	1	52.511	1.7413	0.010
55.282	1.66038	4	0	4	0	55.268	1.6608	0.013
57.747	1.59523	5	0	0	7	57.738	1.5955	0.009

The wavelength used to convert 2θ to d-spacing is 1.54059 Å.

TABLE II. Temperature dependence of cell parameter for lithium *m*-phenylenediamine sulfate.

Temperature (K)	a (Å)	b (Å)	c (Å)	β (°)	Volume (Å^3)	Density (g cm^{-3})	M(20)[a]	F(20)[b]
100	7.8676(8)	6.6234(3)	11.8191(8)	109.398(7)	580.94	1.808	98.4	116.7
150	7.8699(8)	6.6268(6)	11.8240(14)	109.417(10)	581.58	1.806	100.9	132.3
200	7.8712(8)	6.6325(6)	11.8263(11)	109.403(10)	582.34	1.803	76.0	107.9
250	7.8754(9)	6.6370(6)	11.8328(13)	109.410(10)	583.34	1.800	100.9	129.1
300	7.8759(9)	6.6417(4)	11.8378(12)	109.393(10)	584.09	1.798	79.3	108.2
350	7.8812(5)	6.6461(5)	11.8471(11)	109.412(7)	585.27	1.794	93.0	125.2
400	7.8840(5)	6.6501(5)	11.8549(5)	109.429(7)	586.16	1.792	115.8	151.1
450	7.8850(9)	6.6526(6)	11.8584(15)	109.442(20)	586.57	1.790	83.7	114.1
500	7.8853(8)	6.6549(5)	11.8590(11)	109.391(9)	587.01	1.789	68.3	97.2
550	7.8887(6)	6.6582(6)	11.8670(12)	109.402(9)	587.91	1.786	66.6	91.1
600	7.8927(6)	6.6637(7)	11.8775(13)	109.402(9)	589.22	1.782	80.7	96.6

[a]$M(20) = Q_{20}/2\bar{\varepsilon} \ N_{20}$.
[b]$F(20) = N/|\Delta 2\theta N_{poss}|$.

diffraction study. Data were collected using a Bruker D8 VENTURE PHOTO II diffractometer with multilayer mirror monochromatized Mo$K\alpha$ ($\lambda = 0.71073$ Å) radiation at room temperature. Unit-cell refinement and data merging were performed using the APEX3 program, and an absorption correction was applied using the multi-scans method.

III. RESULTS

The PXRD data for LPS at 300 K are given in Table I, which is also contained in the Powder Diffraction File (Gates-Rector and Blanton, 2019), as entry 00-070-1250. All reflections were indexed successfully using the DICVOL14 program (Louër and Boultif, 2014) on a primitive monoclinic system unit cell, with unit-cell parameters $a = 7.8759(9)$ Å, $b = 6.6417(4)$ Å, $c = 11.8378(12)$ Å, $\beta = 109.393(10)°$, and $V = 584.09$ Å^3 at room temperature. A maximum absolute error of 0.013° 2θ was set as the $\Delta 2\theta$ limit for indexing a given observed diffraction line. All k-values in the (0k0) peaks are even, indicating the existence of a 2_1-screw axis along the b-axis. Further check of the symmetry by using CHEKCELL (Laugier and Bochu, 2002) suggests $P2_1/m$ (No. 11) as the possible space group, which is consistent with the systematic absences and with the crystal density. The unit-cell parameters of compound LPS were refined with the program NBS*AIDS83 (Mighell *et al.*,
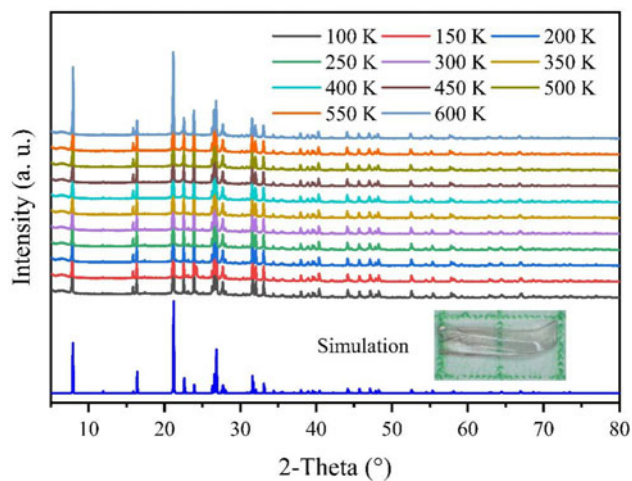
Figure 1. Experimental PXRD patterns at different temperature and simulated ones from the room-temperature crystal structure. Inset: photograph of the crystal of LPS.

TABLE III. Crystallographic data for lithium *m*-phenylenediamine sulfate.

Formula	$Li_2(C_6H_{10}N_2)(SO_4)_2$
Formula weight	316.16 g mol^{-1}
Temperature	293(2) K
Crystal system	Monoclinic
Space group	$P2_1/m$
Unit-cell dimensions	$a = 7.8689(6)$ Å $b = 6.6353(5)$ Å $\beta = 109.385(3)°$ $c = 11.8322(10)$ Å
Volume (Å^3)	582.77(8)
Z	2
Density (calculated)	1.802 g cm^{-3}
$F(000)$	246
Theta range for data collection	2.744–28.331°
Index ranges	$-9 \leq h \leq 10 -8 \leq k \leq 8 -15 \leq l \leq 15$
Independent reflections	1568
Goodness-of-fit on F^2	1.105
R indices [I >2sigma(I)]	$R1 = 0.0319, wR2 = 0.0885$
R indices (all data)	$R1 = 0.0361, wR2 = 0.0922$

1981). The crystal data, density, and figures of merit M20 (de Wolff, 1968) and F20 (Smith and Snyder, 1979) are compiled in Table II.

Powder patterns taken at different temperatures (Figure 1) suggest that LPS has no structural phase transition from 100 to 600 K. The temperature dependences of cell parameters are shown in Figure 2, and the volume expansion of LPS from 100 to 600 K is approximately linear with a coefficient 2.79×10^{-5} K^{-1} (Figure 2). The cell parameters a, b, and c have anisotropic expansion coefficients, which are 6.38×10^{-6} K^{-1}, 1.22×10^{-5} K^{-1}, and 9.88×10^{-6} K^{-1}, respectively, while β is approximately temperature independent.

The crystal structure was solved by direct methods based on the single-crystal diffraction data collected at room temperature, and the structure is refined by the full-matrix method based on F^2 using the SHELXTL software package (Sheldrick, 2008). All non-hydrogen atoms were refined anisotropically, and the H atoms were placed at ideal positions and refined using a "riding" model with $U_{iso} = 1.2\ U_{eq}$ (C) or $U_{iso} = 1.5 U_{eq}$ (N). The crystallographic data for lithium *m*-phenylenediamine sulfate are listed in Table II, the fractional atomic coordinates and equivalent isotropic displacement parameters are given in Table III. It is confirmed that the compound crystallizes in space group $P2_1/m$ with formula unit $Z = 2$. Both sulfate groups and *m*-phenylenediamine molecules are intact and are fully ordered in the compound (Figure 3). Different from the six coordination of metals in HOIPs, each lithium ion in LPS is connected to four SO_4^{2-} forming a slightly distorted tetrahedron with Li–O bond lengths from 1.958 to 1.995 Å and O–Li–O bond angles from 106.49° to 120.03°. Such distorted [Li(SO$_4$)$_4$]
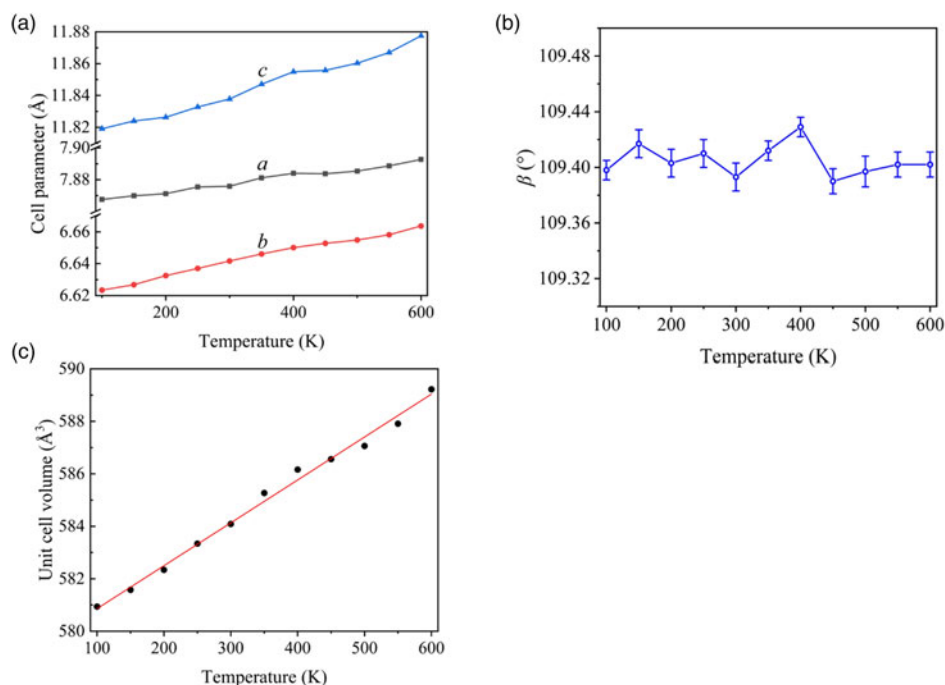

Figure 2. Change of (a) cell parameters, (b) β, and (c) volume with temperature. The error bars in (a) and (c) are too small to be displayed.
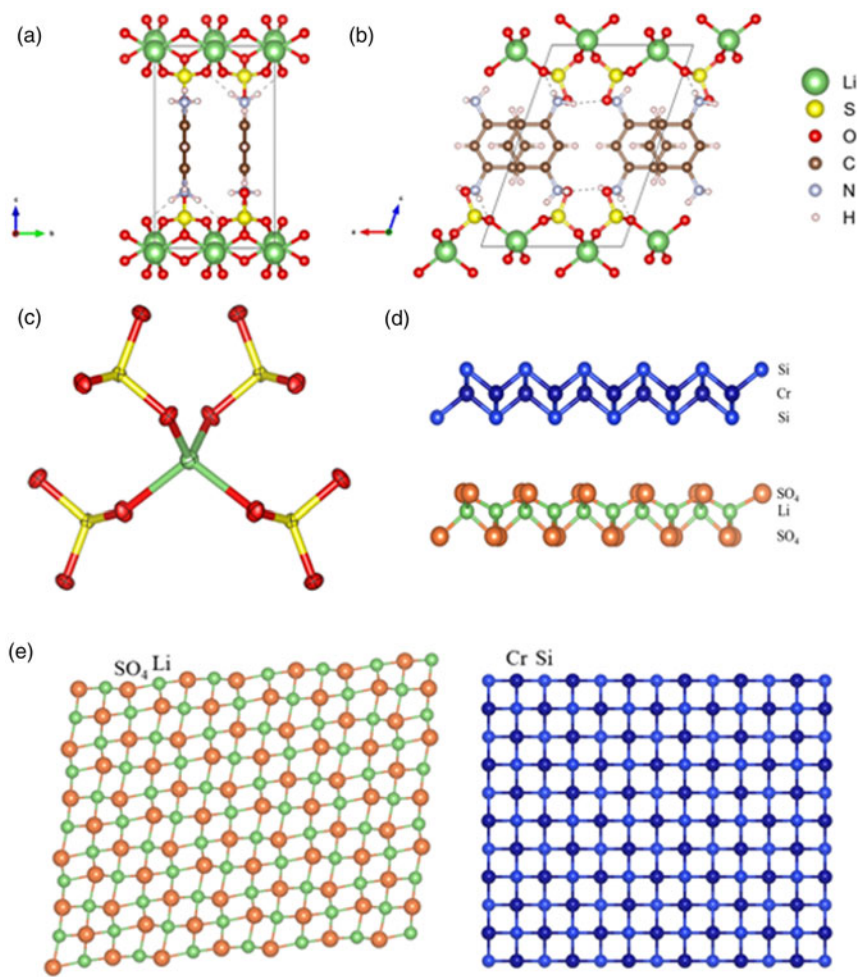
Figure 3. Projections of LPS along (a) *a*-axis and (b) *b*-axis, dashed lines represent hydrogen bonds. (c) The coordination environment of the Li$^+$ with displacement ellipsoids drawn at the 50% probability level. (d) Projections along the direction parallel to the anti-fluorite layers both in ThCr$_2$Si$_2$ and LPS. (e) Projections along the direction perpendicular to the anti-fluorite layers both in ThCr$_2$Si$_2$ and LPS. For simplicity, the sulfates are replaced by orange balls at the center of mass of the sulfates.

tetrahedrons are also observed in Li$_2$SO$_4$ (Albright, 1933). The lithium and SO$_4^{2-}$ form quasi-two-dimensional anti-fluorite layers parallel to the *ab* plane [Figures 3(d) and 3(e)], and the interlayer distance is 11.161 Å (*c·sin β*). Hydrogen atoms on amino group in *m*-phenylenediamine are connected to oxygen atoms of SO$_4^{2-}$ through hydrogen bonds. In this way, organic molecules lie between [LiSO$_4$] layers, with their benzene rings perpendicular to the *b*-axis. Similar structures were recently found in FeSe-based superconductors such as Na$_{0.39}$(C$_2$H$_8$N$_2$)$_{0.77}$Fe$_2$Se$_2$ (Jin *et al*., 2017), Na$_{0.35}$(C$_3$H$_{10}$N$_2$)$_{0.426}$Fe$_2$Se$_2$ (Fan *et al*., 2018), and Li$_x$(C$_2$H$_8$N$_2$)$_y$Fe$_2$Se$_2$ (Zhao *et al*., 2019), in which alkali metals and organic molecules are co-inserted in between anti-fluorite FeSe layers. It should be noted that although protonated *m*-phenylenediamine is a polar cation with an electric dipole moment along the center of two nitrogen atoms and benzene ring, the two *m*-phenylenediamine molecules in the unit cell of LPS have opposite electric dipole moments (along [100] and [$\bar{1}$00]), maintaining a net-zero moment in the whole structure. There are one-dimensional channels between the *m*-phenylenediamine and extending along the *a*-axis. The size of the channels is around 7.8 Å × 3.3 Å, which may be used to selectively filter out some small molecules (Tables IV and V).

IV. CONCLUSION

The lithium *m*-phenylenediamine sulfate was prepared under aqueous solution conditions. The incorporation of

TABLE IV. Fractional atomic coordinates and equivalent isotropic displacement parameters for lithium *m*-phenylenediamine sulfate.

Atom	x	y	Z	U_{iso}
S1	0.87997(7)	0.2500	0.85046(4)	0.01325(15)
S2	0.52961(7)	0.2500	0.14956(4)	0.01327(15)
Li1	0.7627(4)	0.0003(4)	0.0253(2)	0.0199(5)
O1	0.3427(2)	0.2500	0.06401(14)	0.0195(3)
O2	0.62426(15)	0.06856(18)	0.13026(10)	0.0210(3)
O3	0.99403(15)	0.06859(18)	0.86967(10)	0.0212(3)
O4	0.7788(2)	0.2500	0.93613(15)	0.0196(3)
O5	0.7532(2)	0.2500	0.72740(15)	0.0251(4)
O6	0.5259(2)	0.2500	0.27253(15)	0.0247(4)
N1	0.1808(3)	0.2500	0.27868(17)	0.0188(4)
N2	0.4021(3)	0.2500	0.72133(17)	0.0187(4)
C1	−0.0591(3)	0.2500	0.5000(2)	0.0242(5)
C2	0.0820(3)	0.2500	0.6071(2)	0.0213(5)
C3	−0.0251(3)	0.2500	0.3929(2)	0.0213(5)
C4	0.1515(3)	0.2500	0.39390(19)	0.0161(4)
C5	0.2576(3)	0.2500	0.6060(2)	0.0158(4)
C6	0.2961(3)	0.2500	0.5000(2)	0.0166(4)
H1	−0.1773	0.2500	0.5000	0.029
H2	0.0594	0.2500	0.6794	0.026
H3	−0.1199	0.2500	0.3205	0.026
H4	0.4143	0.2500	0.5000	0.020
H5	0.2985	0.2500	0.2905	0.028
H6	0.1309	0.1405	0.2376	0.028
H7	0.1309	0.3595	0.2376	0.028
H8	0.5080	0.2500	0.7095	0.028
H9	0.3933	0.3595	0.7625	0.028
H10	0.3933	0.1405	0.7625	0.028

TABLE V. Selected bond lengths (Å) and bond angles (°) for lithium *m*-phenylenediamine sulfate.

	Bond lengths		Bond angles
Li1–O1	1.995(3)	O1–Li1–O2	107.91(16)
Li1–O2	1.958(4)	O1–Li1–O3	106.77(14)
Li1–O3	1.959(3)	O1–Li1–O4	120.03(13)
Li1–O4	1.991(3)	O2–Li1–O3	106.49(12)
		O2–Li1–O4	106.88(15)
		O3–Li1–O4	108.04(16)

protonated organic amines, Li^+ metal cations with four SO_4^{2-} successfully stabilized a compound with organic amines intercalated in-between anti-fluorite type layers. The crystal structure was determined from the X-ray single-crystal diffraction data. The title compound possesses a layered monoclinic structure without phase transition between 100 to 600 K, and the volume expansion coefficient is determined to be 2.79×10^{-5} K^{-1} based on the PXRD data.

V. DEPOSITED DATA

The Crystallographic Information System files $Li_2(C_6H_{10}N_2)(SO_4)_2$-1.cif (for the PXRD data) and $Li_2(C_6H_{10}N_2)(SO_4)_2$-2.cif (for the single-crystal data) were deposited with the ICDD. The data files can be requested at info@icdd.com.

Albright, J. G. (**1933**). "The crystal structure of lithium sulphate," Z. Kristallogr. Cryst. Mater. **84**, 252–258.

Ban, Z. and Sikirica, M. (**1965**). "The crystal structure of ternary silicides ThM2Si2 (M = Cr, Mn, Fe, Co, Ni and Cu)," Acta Crystallogr. **18**, 594–599.

Chen, X. G., Song, X. J., Zhang, Z. X., Li, P. F., Ge, J. Z., Tang, Y. Y., Gao, J. X., Zhang, W. Y., Fu, D. W., You, Y. M., and Xiong, R. G. (**2020**). "Two-dimensional layered perovskite ferroelectric with giant piezoelectric voltage coefficient," J. Am. Chem. Soc. **142**, 1077–1082.

de Wolff, P. M. (**1968**). "A simplified criterion for the reliability of a powder pattern indexing," J. Appl. Crystallogr. **1**, 108–113.

Fan, X., Deng, J., Chen, H., Zhao, L., Sun, R., Jin, S., and Chen, X. (**2018**). "Nematicity and superconductivity in orthorhombic superconductor Na0.35(C3N2H10)0.426Fe2Se2," Phys. Rev. Mater. **2**, 114802.

Gates-Rector, S. D., and Blanton, T. N. (**2019**). "The powder diffraction file: a quality materials characterization database," Powd. Diffr. **34**, 352–360.

Hu, Y., Florio, F., Chen, Z., Phelan, W. A., Siegler, M. A., Zhou, Z., Guo, Y., Hawks, R., Jiang, J., Feng, J., Zhang, L., Wang, B., Wang, Y., Gall, D., Palermo, E. F., Lu, Z., Sun, X., Lu, T. M., Zhou, H., Ren, Y., Wertz, E., Sundararaman, R., and Shi, J. (**2020**). "A chiral switchable photovoltaic ferroelectric 1D perovskite," Sci. Adv. **6**, eaay4213.

Hurd, J. A., Vaidhyanathan, R., Thangadurai, V., Ratcliffe, C. I., Moudrakovski, I. L., and Shimizu, G. K. (**2009**). "Anhydrous proton conduction at 150 degrees C in a crystalline metal-organic framework," Nat. Chem. **1**, 705–710.

Jin, S., Fan, X., Wu, X., Sun, R., Wu, H., Huang, Q., Shi, C., Xi, X., Li, Z., and Chen, X. (**2017**). "High-Tc superconducting phases in organic molecular intercalated iron selenides: synthesis and crystal structures," Chem. Commun. **53**, 9729–9732.

Ju, M. G., Dai, J., Ma, L., Zhou, Y., and Zeng, X. C. (**2018**). "Zero-dimensional organic-inorganic perovskite variant: transition between molecular and solid crystal," J. Am. Chem. Soc. **140**, 10456–10463.

Laugier, J. and Bochu, B. (**2002**). *CHEKCELL, LMGP-Suite of Programs for the Interpretation of X-ray Experiments*. ENSP/Laboratoire des Matériaux et du Génie Physique, BP 46. 38042 Saint Martin d'Hères, France. Available at: http://www.inpg.fr/LMGP and http://www.ccp14.ac.uk/tutorial/lmgp/.

Li, W., Wang, Z., Deschler, F., Gao, S., Friend, R. H., and Cheetham, A. K. (**2017**). "Chemically diverse and multifunctional hybrid organic–inorganic perovskites," Nat. Rev. Mater. **2**, 16099.

Liao, W. Q., Zhao, D., Tang, Y. Y., Zhang, Y., Li, P. F., Shi, P. P., Chen, X. G., You, Y. M., and Xiong, R. G. (**2019**). "A molecular perovskite solid solution with piezoelectricity stronger than lead zirconate titanate," Science **363**, 1206–1210.

Llabresixamena, F., Abad, A., Corma, A., and Garcia, H. (**2007**). "MOFs as catalysts: activity, reusability and shape-selectivity of a Pd-containing MOF," J. Catal. **250**, 294–298.

Louër, D. and Boultif, A. (**2014**). "Some further considerations in powder diffraction pattern indexing with the dichotomy method," Powd. Diffr. **29**, S7–S12.

Mighell, A. D., Hubbard, C. R., and Stalick, J. K. (**1981**). *NBS*AIDS80, A FORTRAN Program for Crystallographic Data Evaluation*. NBS (U.S.) Technical Note 1141 (U.S. Department of Commerce (NBS*Aids83 is upgraded from NBS*Aids80), Gaithersburg, MD).

Rosi, N. L., Eckert, J., Eddaoudi, M., Vodak, D. T., Kim, J., O'Keeffe, M., and Yaghi, O. M. (**2003**). "Hydrogen storage in microporous metal-organic frameworks," Science **300**, 1127–1129.

Saparov, B. and Mitzi, D. B. (**2016**). "Organic-iorganic perovskites: structural versatility for functional materials design," Chem. Rev. **116**, 4558–4596.

Sheldrick, G. M. (**2008**). "A short history of SHELX," Acta Crystallogr. A **64**, 112–122.

Smith, G. S. and Snyder, R. L. (**1979**). "FN: a criterion for rating powder diffraction patterns and evaluating the reliability of powder-pattern indexing," J. Appl. Crystallogr. **12**, 60–65.

Wang, C., Zhang, T., and Lin, W. (**2012**). "Rational synthesis of noncentrosymmetric metal-organic frameworks for second-order nonlinear optics," Chem. Rev. **112**, 1084–1104.

Yanai, N., Kitayama, K., Hijikata, Y., Sato, H., Matsuda, R., Kubota, Y., Takata, M., Mizuno, M., Uemura, T., and Kitagawa, S. (**2011**). "Gas detection by structural variations of fluorescent guest molecules in a flexible porous coordination polymer," Nat. Mater. **10**, 787–793.

Zhao, L., Wang, D., Huang, Q., Wu, H., Sun, R., Fan, X., Song, Y., Jin, S. and Chen, X. (**2019**). "Structural evolution and phase diagram of the superconducting iron selenides Lix(C2H8N2)yFe2Se2(x=0~0.8)," Phys. Rev. B. **99**, 094503.